



Noise characterization of a soliton mode locking laser

Carlo Bevilacqua,

Università degli studi di Bari, Italy

Supervisor: Axel Ruehl

September 8, 2015

Abstract

Noise performances of a laser system is of great importance for most applications. It has been observed that in a soliton mode locking laser noise tends to concentrate in some regions of its optical spectrum. This project aims to further investigate this phenomenon by measuring the noise distribution along the optical spectrum of a low noise soliton oscillator. The experimental data and possibly a future simulation can help in understanding the physical origin of this noise distribution and to eventually exploit it for noise reduction.

Contents

| | |
|---|-----------|
| 1. Introduction | 3 |
| 1.1. Setup description | 3 |
| 2. Dispersion measurement with Kelly sidebands | 4 |
| 3. Noise measurement | 6 |
| 3.1. Definition of RIN | 6 |
| 3.2. Detector design | 7 |
| 3.3. Spectrally resolved RIN measurement | 7 |
| 4. Transfer function | 8 |
| 5. Results and discussion | 9 |
| A. Detector noise | 12 |

1. Introduction

Soliton mode locking lasers have a great importance for their compactness and high repetition rate, especially in telecommunication system.

It has been known for decades that the optical spectrum of such solitons gets some sidebands, named Kelly sidebands after the first person who explained their physical origin [2], because of the gain and losses in the laser cavity.

Recently [4] it has been observed that the noise of the laser tends to concentrate in these sidebands: figure 1 shows how differently pump noise reflects on the main soliton and on the sidebands.

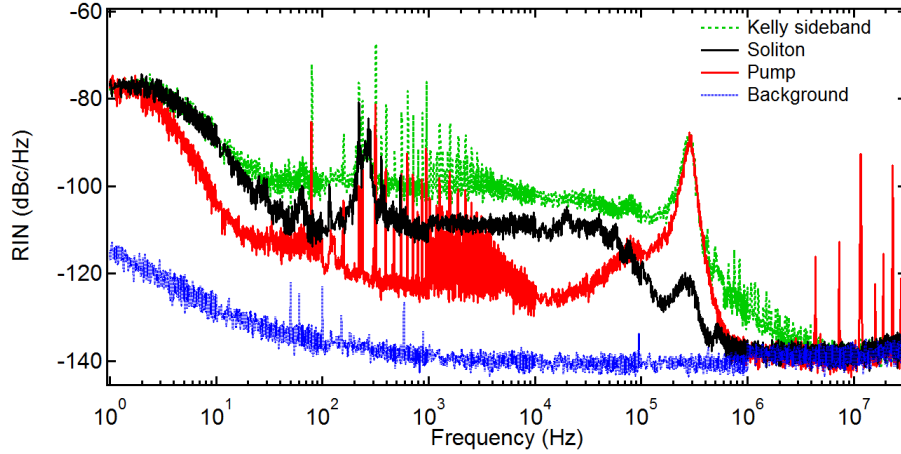


Figure 1: Noise measurements on an Holium-doped fiber oscillator that shows how the noise of the pump is differently distributed on the optical spectrum of the soliton.

The main aim of this project is to take similar measurements with an erbium-doped fiber laser having a less noisy pump and to resolve the noise distribution along the optical spectrum with a finer resolution. To achieve this purpose great care should be taken in designing the detector to have a low noise floor and in reducing the source of external noise e.g. due to vibration of the fiber and optics.

Moreover fiber dispersion at the operating wavelength of the laser needs to be measured to provide enough parameters for simulating the noise performance and compare it with the experimental data.

1.1. Setup description

In figure 2 is shown schematically the laser used for the measurement. It consists of a ring fiber resonator with an Erbium doped fiber as a gain medium pumped with a 890 nm laser diode. The saturable absorber is realized by exploiting intensity dependent polarization change of light due to self phase modulation. The isolator is the actual

absorber because it blocks light that is linearly polarized in a specific direction. To start the mode locked operation, the polarization controller is adjusted so that light with highest intensity has the right polarization to pass through the isolator. Light with an orthogonal polarization, that would be blocked by the isolator, can exit the cavity through the polarizing beam splitter and is used as output of the laser.

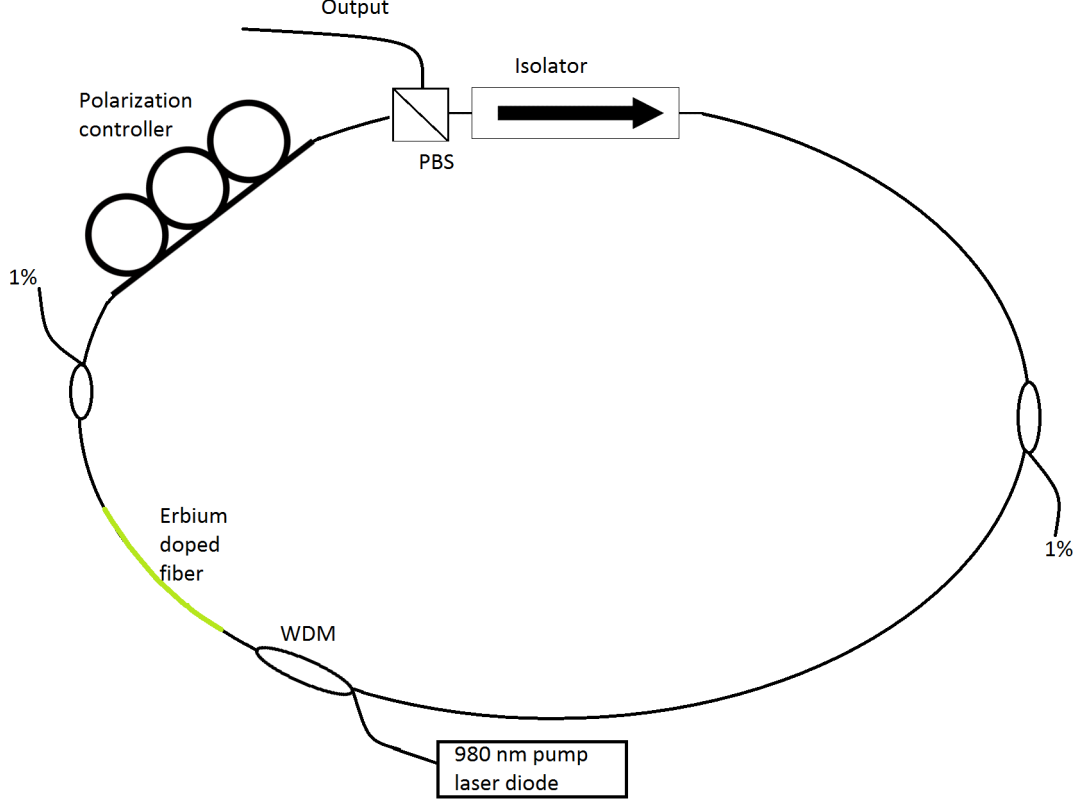


Figure 2: Fiber soliton laser

2. Dispersion measurement with Kelly sidebands

Fiber dispersion is an important parameter for simulation. In this paragraph is described a measurement approach based on Kelly sidebands.

In figure 4 is shown the optical spectrum of the laser in log scale. Apart from the central part of the spectrum, peaked at 1566 nm, that corresponds to the soliton, several sidebands can be observed.

As described in [3], they arise from a resonant process between the soliton and the dispersive wave that is originated from the soliton because of gain and losses in the laser cavity. The resonance condition can be written:

$$N = -\frac{1}{4\pi}L\beta_2(\Delta\omega_N^2 + \tau_0^{-2}) - \frac{1}{12\pi}L\beta_3\Delta\omega_N^3 \quad (1)$$

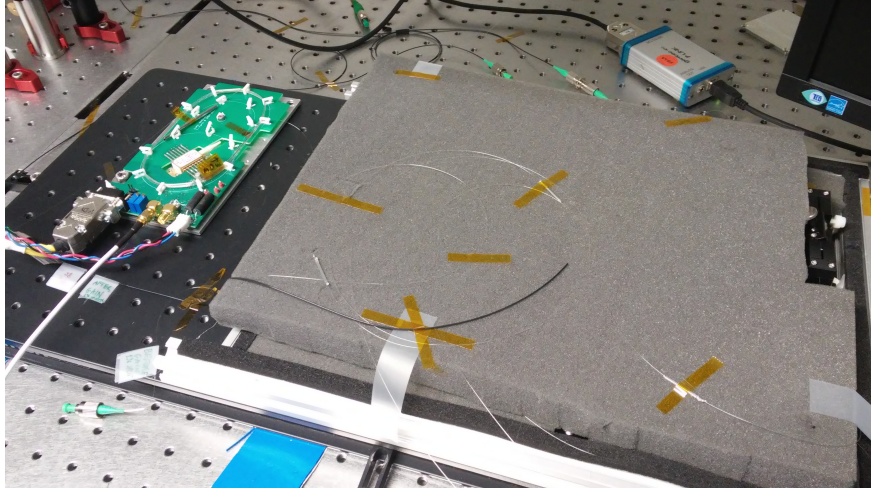


Figure 3: Picture of the soliton laser. The ring cavity is under the foam, used to reduce fiber vibration. On the right is the polarization controller. On the left is the board used to drive and modulate the pump laser diode.

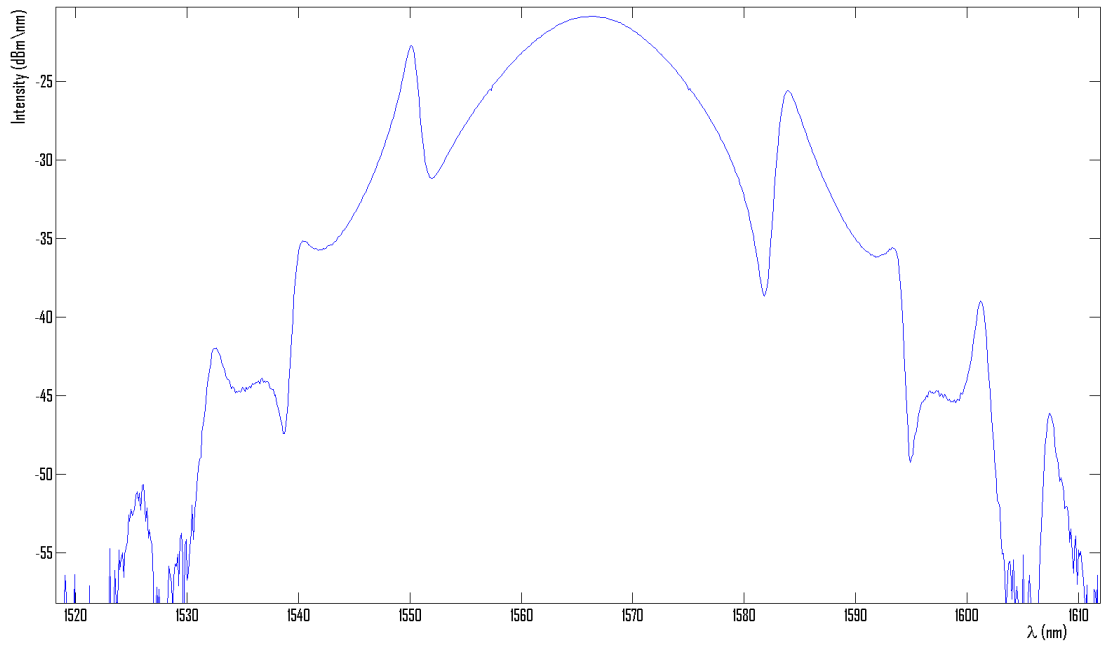


Figure 4: Optical spectrum (log scale) of the laser.

where $N = 1, 2, \dots$, β_2 and β_3 are the second and third order dispersion, L is the fiber length, τ_0 is the soliton length and $\Delta\omega_N$ is the angular frequency difference between the soliton and the N^{th} sideband. Neglecting third order dispersion β_3 , equation 1 becomes

$x = aN + b$ where $a = -\frac{4\pi}{L\beta_2}$, $b = -\frac{1}{\tau_0^2}$ and $x = \Delta\omega_N^2 = \frac{4\pi^2 c^2}{\lambda_0^4} \Delta\lambda_N^2$

The sideband positions were determined by fitting their maxima with a second order polynomial and the center soliton was fitted with a gaussian. Then x was calculated as explained before. The results are shown in figure 5. The fit of the data with a line gave two values for the dispersion $L\beta_2$ and the soliton length τ_0 and the weighted arithmetic mean of the two resulted in:

$$L\beta_2 = (-0.048 \pm 0.003)ps^2 \quad (2)$$

$$\tau_0 = 104 \pm 42fs \quad (3)$$

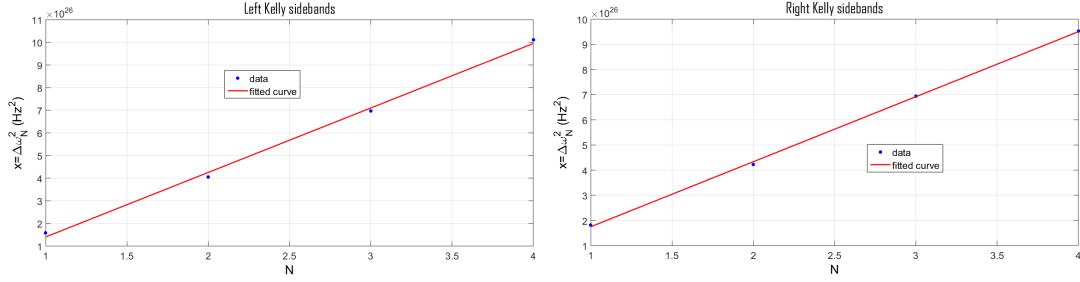


Figure 5: Experimental data and fit of Kelly sidebands displacement with respect to central soliton at lower wavelengths (left) and at higher wavelengths (right).

3. Noise measurement

3.1. Definition of RIN

A noisy laser has a power that randomly fluctuates in time. This correspond, in frequency domain, to a power spectral domain $P_{opt}(f)$ of the noise. It is common to normalize $P_{opt}(f)$ to the DC power, in order to have a value independent from the mean power that makes it easier to compare different laser. The relative intensity noise is defined as:

$$RIN = \left(\frac{P_{opt}(f)}{P_{opt,DC}} \right)^2 \quad (4)$$

In a photodiode the photocurrent is proportional to the optical power shining on it thus, if a transimpedance amplifier is used, the output voltage is proportional to the optical power. If the power spectral density $P(f)$ of the photodetector is measured with a vector analyser (that has an input impedance of 50Ω), the RIN can be calculated as:

$$RIN = \frac{P(f)}{\frac{v_{DC}^2}{50\Omega}} \quad (5)$$

where v_{DC} is the DC voltage that can be measured with a multimeter. It is common to express the RIN as logarithmic value below carrier (dBc/Hz):

$$RIN[\frac{dBc}{Hz}] = 10 \lg(RIN) \quad (6)$$

If the RIN is integrated in a certain bandwidth and square rooted, a r.m.s. value of RIN is obtained that is usually expressed in percent:

$$\frac{\delta P}{\overline{P}}|_{r.m.s.} = \sqrt{\int_{f_1}^{f_2} RIN(f) df} \quad (7)$$

3.2. Detector design

The photoreceiver must be designed to have a noise floor that is below the shotnoise level. In fact the laser noise should approach this level at high frequency where no other sources of noise are present.

The shotnoise scales as the square root of the optical power shooting on the detector and, in principle, it is easier to reach the previous condition with higher power. However higher power requires higher dynamic range for the detector and can make it operating in nonlinear regime thus making the noise measurement not reliable.

The approach used is to work at the maximum power before saturation and calculate the optimal gain of amplifier to fulfill the requirements. In the appendix A is explained how to calculate the noise of the detector.

The photodiode used was a fiber pigtailed photodiode by AFR having a dark current of 2nA (70C, -5V bias), $R_d = 2.5G\Omega$ and R_s is usually few ohms thus negligible with respect to R_d . The datasheet doesn't give any information about saturation current: it was estimated by observing when the ratio between the optical power shining on the photodiode and the output voltage starts to decrease, both in terms of DC and AC components.

It was calculated that the feedback resistor should be above $2.4k\Omega$ in order to have a shotnoise limited measurement.

3.3. Spectrally resolved RIN measurement

A numerical simulation performed with generic parameters on a soliton oscillator (figure 6) showed a fine structure in the noise distribution along the optical spectrum of the soliton: it consists of a dip in the center with symmetric lobes and sharp peaks in the sidebands.

To resolve this trend experimentally is necessary to measure the noise in a narrow region of the optical spectrum. To achieve this the setup shown in figure 7 was used. A fiber collimator collimates the light coming out from the main output of the laser. An isolator is needed to prevent feedback in the laser cavity that would interfere with mode locking operation. A quarter and a half waveplate can adjust the polarization of light so that

is linearly polarized in the correct direction to pass through the isolator without attenuation. An half waveplate sets the polarization so that grating efficiency is maximum. A nanoblock couples back in fiber the light dispersed by the grating within small angles that correspond to a bandwidth of a couple of nm, even without a slit. The wavelength tuning is achieved by rotating the grating.

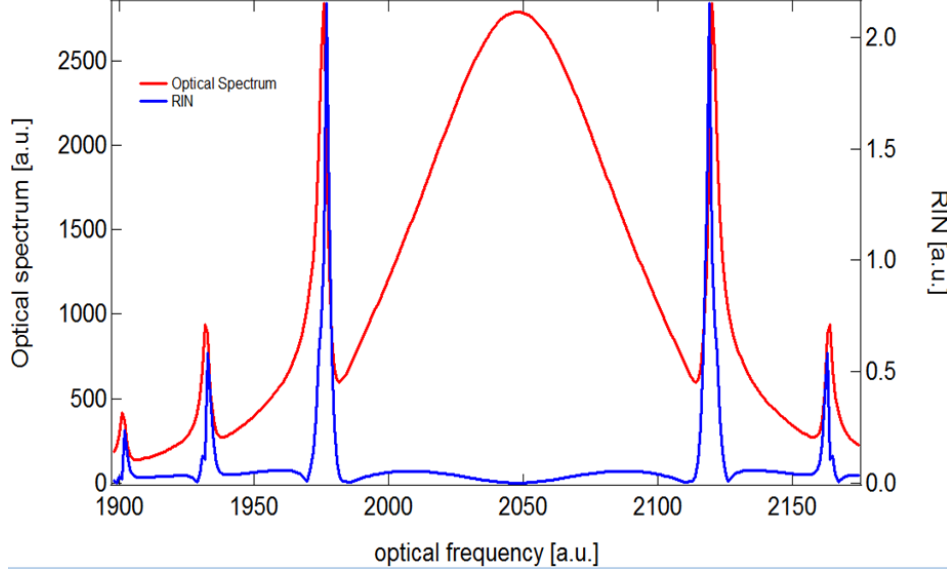


Figure 6: Noise distribution predicted by a simulation on a generic soliton oscillator.

4. Transfer function

To understand how noise at a given frequency in the pump is transferred to the laser, one can introduce on purpose modulation of known amplitude on the pump and measure amplitude modulation of the laser.

To modulate the pump at MHz frequency the circuit shown in figure 9 was used: the LD driver supplies a constant current that splits between the transistor and the diode. The signal on the base of the transistor establishes the current flowing in its collector thus, by difference, the current in the diode. Using this strategy the current can be modulated at high frequency, the limit being the cutoff frequency of the transistor.

The signal to modulate the pump was generated by the vector analyzer. To monitor the modulation of the pump a 1% splitter was added between the pump output and the WDM. Light from the 1% port was collimated with a nanoblock and focused on a freespace photodiode. The signals from both the pump and laser photodiode were fed into channel 1 and 2 of the vector analyzer. It can directly calculate the transfer function both in amplitude and phase while sweeping the modulation frequency.

A block diagram of the setup used to measure the transfer function is shown in figure 10.

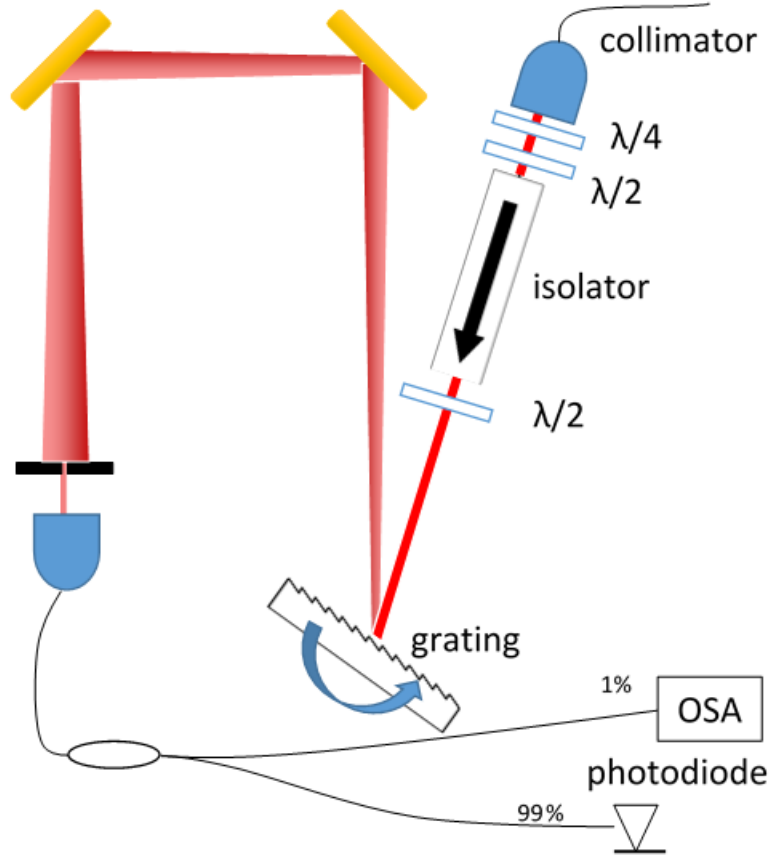


Figure 7: Setup used to spectrally resolve the noise of the laser. The wavelength tuning is achieved by rotating the grating

5. Results and discussion

In figure 11 is shown the RIN measured at the center of the optical spectrum and at both Kelly sidebands. The feedback resistor used for the transimpedance amplifier was $2.872k\Omega$ that, according to calculation, should have made the system shotnoise limited. However it was out of few dB mainly due to wrong estimation of saturation current. The integrated r.m.s. RIN, as defined in 7, from 100 Hz to 10 MHz is 0.097% in the left sideband, 0.027% in the center and 0.080% in the right sideband.

In the first decade of frequency axis, that is the audio region, the noise is originated mainly from the vibrations: a sound in the laboratory could make the noise level rise; a possible improvement would be to box also the free space part of the setup. At very high frequency all the noise is expected to reach the shotnoise level (or the noise background of the detector if the latter is limiting); in fact starting from about 2MHz the noise of the sidebands starts to drop and tends to the detector noise floor. The maximum **noise reduction** between the center and the sidebands is **24 dB** at about 2kHz, in the worst case. At intermediate frequency the noise reduction is lower because of noise floor of

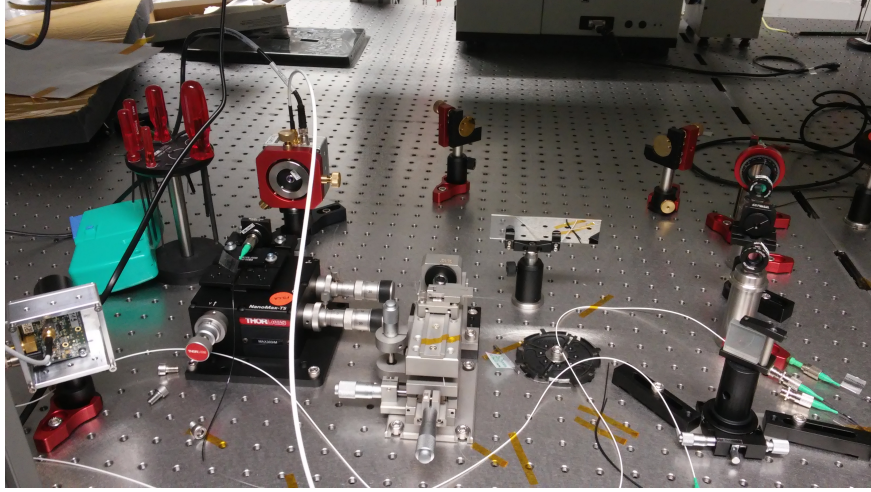


Figure 8: Picture of setup schematically shown in figure 7.

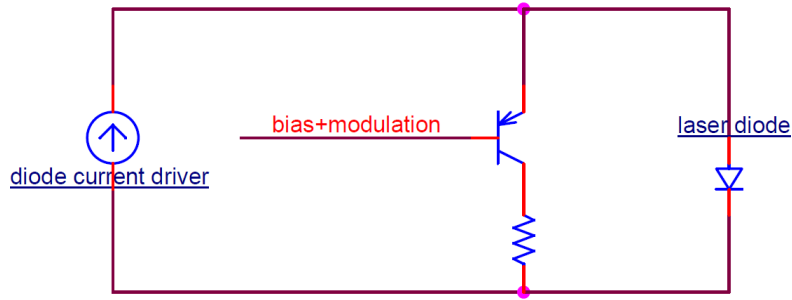


Figure 9: Circuit used to modulate the pump diode laser.

the measurement system. To confirm this hypothesis the transfer function at the same regions of the spectrum was measured, so that noise at a certain frequency is increased and can eventually emerge from the background.

The r.m.s. modulation of the pump was 1.4% of the mean pump power at 1KHz. The transfer function (figure 5) shows the same suppression between center and sidebands as the RIN. The fact that the frequency dependence of transfer function is the same between the different spectral areas suggests that the damping of laser modulation at high frequency is related to dynamics in the gain fiber that affects equally the gain of every wavelength in the laser cavity. At frequency above hundreds of KHz the modulation of the laser became smaller and smaller and can no more be distinguished from the noise background; this is also confirmed by the phase of the transfer function that starts to vary randomly between -180 and 180.

In figure 5 is shown the transfer function at some frequency for 16 different point in the optical spectrum. The choice of a log scale was made to make evident the fine structure in the soliton that wouldn't be discernible in a linear scale due to the > 20 dB

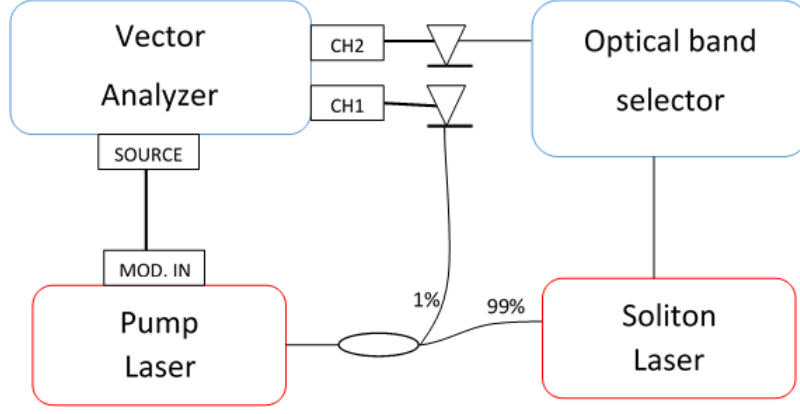


Figure 10: Block diagram of the setup used to measure the transfer function. 'Optical band selector' is the setup shown in figure 7

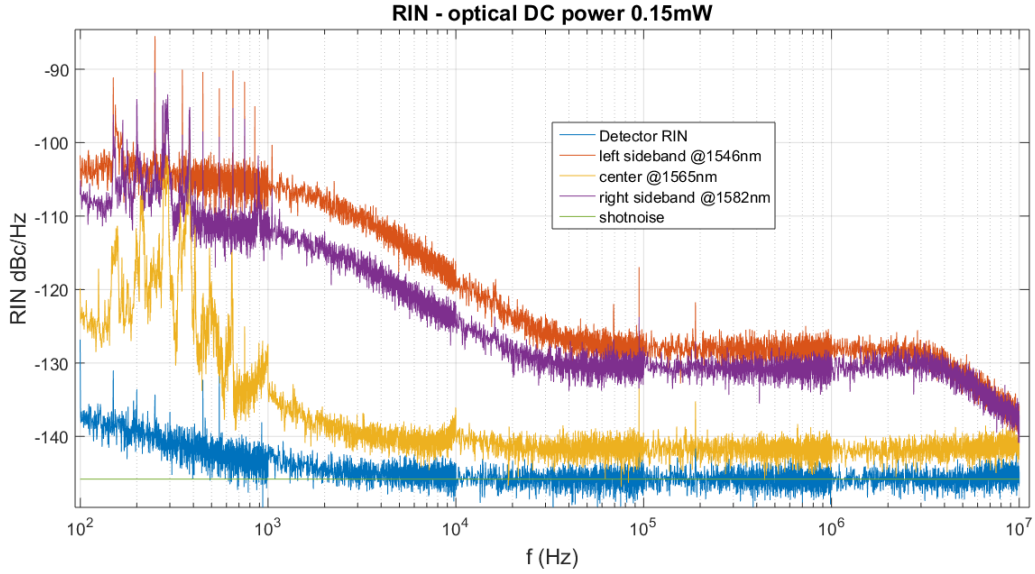
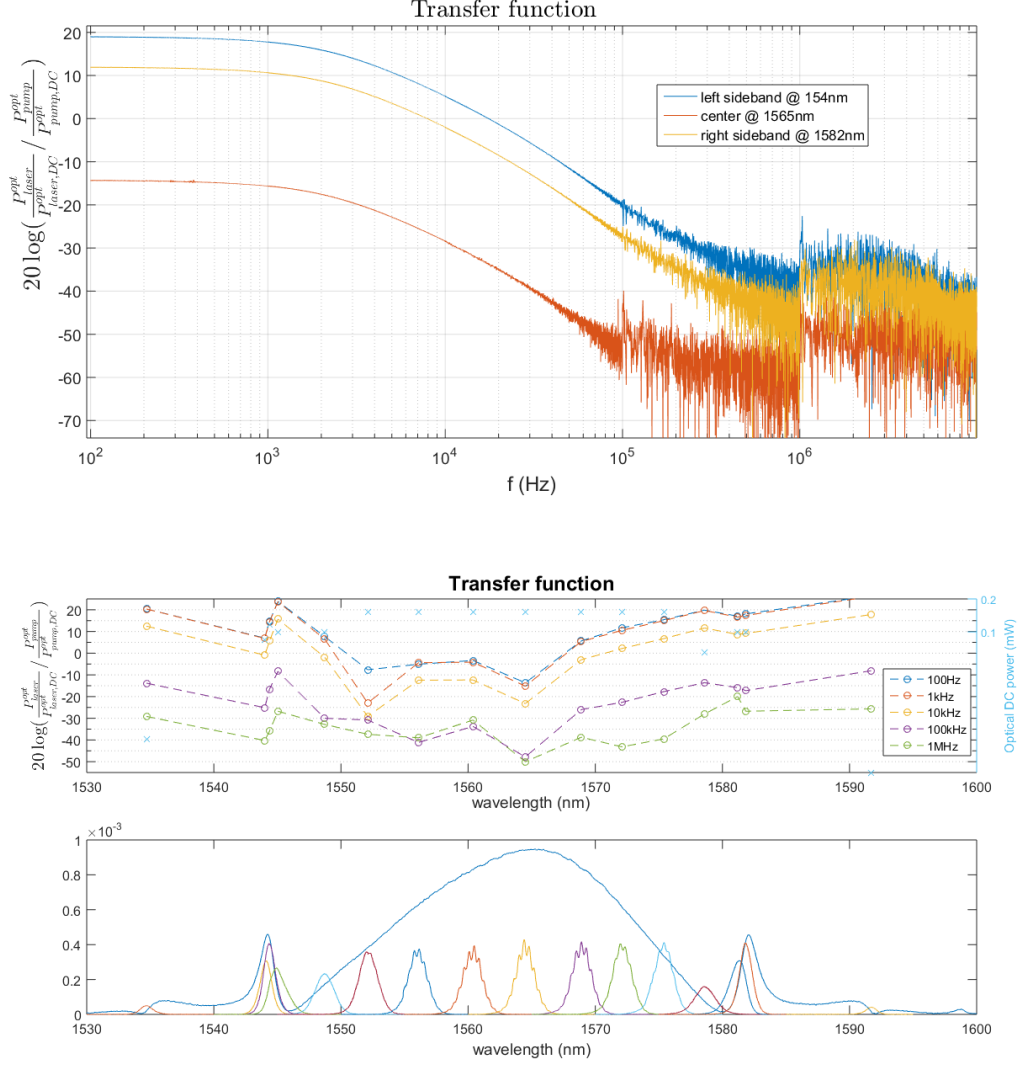


Figure 11: RIN, as defined in 6, of the spectrum measured at the center of the spectrum and at both Kelly sidebands.

suppression between soliton and central part.

The trend is quite similar to what was expected by the simulation. However some asymmetries are present and the peak of noise in the right sideband is much less evident than the one in the left. This could be due to thermal fluctuation: the vector analyzer was blowing on the setup and the measurements on the right were taken roughly a couple of hours after the first ones. To check if this is the case another measurement is planned with more care on setup isolation and possibly with a finer resolution that can help in understanding if other effects are present.



A. Detector noise

Noise measurement represents a difficult task because of the extraordinary noise performance of lasers and high peak-to-average ratio of mode-locked lasers. Therefore the choice of the detector is a fundamental step in the measurement process.

In this appendix are summarized the requirements in terms of dynamic range and the contributions to the noise of the detector in the case of a transimpedance amplifier, as discussed in [5].

To give an estimation of the dynamic range required, a CW laser is considered. The smallest fluctuations detectable are limited by the shotnoise level, while the maximum amplitude noise is approximately equal to the average laser power. Therefore the **dynamic range** is:

$$DR = \frac{i_0}{2qB} \quad (8)$$

where $q = 1.6 \cdot 10^{-19}C$ is the electron charge, B is the receiver bandwidth and i_0 is the average photocurrent.

As far as noise is considered, in figure 12 is shown the equivalent circuit (including the noise sources) of a photodiode whose current signal is amplified by a transimpedance amplifier, which is the best design for most applications. The photodiode dark current i_d , flowing in its internal resistance $R_s + R_d$, is the first source of noise because of the shotnoise associated with it. However this is usually small compared to the op-amp input noise voltage e_n and current i_n and the Johnson noise associated with resistors, especially the feedback resistor R_f . Because every noise source is independent from others, the total noise is the mean square:

$$\overline{v_0^2} = \left[\frac{2qi_d R_d^2}{(R_s + R_d)^2} + \frac{4kT}{R_s + R_d} + \overline{i_n^2} + \frac{4kT}{R_f} \right] R_f^2 + \overline{e_n^2} \left(1 + \frac{R_f}{R_s + R_d} \right)^2 \quad (9)$$

This is the voltage noise per 1 Hz bandwidth. It seems to be white noise however e_n and i_n usually depend on frequency.

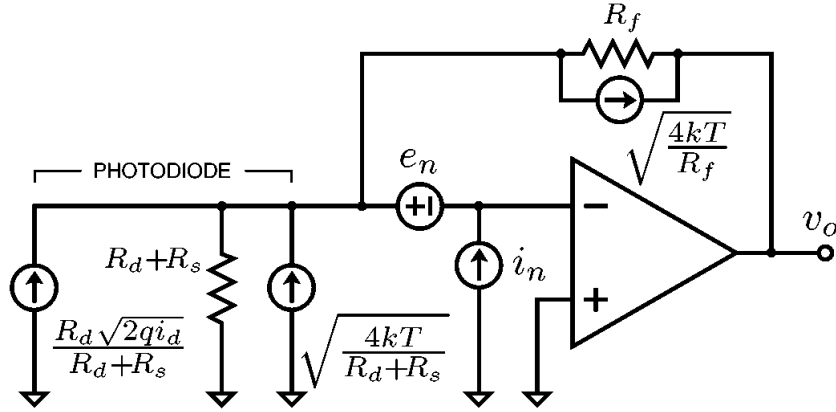


Figure 12: Equivalent circuit of a transimpedance amplifier driven by a photodiode including noise sources.

References

- [1] https://www.rp-photonics.com/relative_intensity_noise.html
- [2] Kelly, S.M.J., "Characteristic sideband instability of periodically amplified average soliton," in Electronics Letters , vol.28, no.8, pp.806-807, 9 April 1992
- [3] Dennis, Michael L., and Irl N. Duling III. "Experimental study of sideband generation in femtosecond fiber lasers." Quantum Electronics, IEEE Journal of 30.6 (1994): 1469-1477.
- [4] P. Li, A. Ruehl, C. Bransley, and I. Hartl, "Passively Mode-locked Holmium-doped Fiber Oscillators Optimized for Ho:YLF Amplifier Seeding," in CLEO: 2015, OSA Technical Digest (online) (Optical Society of America, 2015), paper STh1L.4.
- [5] Scott, Ryan P., Carsten Langrock, and Brian H. Kolner. "High-dynamic-range laser amplitude and phase noise measurement techniques." Selected Topics in Quantum Electronics, IEEE Journal of 7.4 (2001): 641-655.